JOHN C. PRICE*
NASA/Goddard Space Flight Center
Greenbelt, MD 20771

The Contribution of Thermal Data in Landsat Multispectral Classification

Thermal data provide additional information but must be used with care.

ABSTRACT: *Thermal data from the Landsat-3 Multispectral Scanner (MSS) are used in conjunction with visible near-infrared data associated with a scene in New York State in order to assess the contribution of thermal data in classification. Despite limitations resulting from poor thermal resolution (~±1.5C), a spatial resolution 1/9 of the other bands, and instrumentation problems, the thermal data are shown by principal component analysis to provide additional information representing a potential discriminating factor for multispectral classification. However, analysis shows that this information is not readily associated with that in the visible near-infrared for identification of surface types and may lead to misinterpretation or spurious classification unless considerable caution is exercised. A physical explanation is suggested involving thermal fluxes at the Earth's surface.*

INTRODUCTION

THE VALUE of Landsat multispectral scanner data for discrimination of some rock and mineral types, vegetation cover, crop discrimination, land-use evaluation, etc., has been fully established in the scientific literature (Harding and Scott, 1978; Rabchevsky *et al.*, 1979; Scarpace *et al.*, 1979; Thompson and Wehmanen, 1979). This conclusion results from the fact that the multispectral data provide a number of independent measurements of the reflective characteristics of each surface element observed. These spectral measurements yield a descriptor, or "spectral signature," which is a function of the type of area observed. The identification of spectral signatures (e.g., grass, snow, sand, and water all have quite different signatures) provides the basis for classification; i.e., partitioning an image into a number of categories representing the different surface types present. Studies with data from Landsats 1 and 2 have shown that the classification is sometimes not unique, as several distinct surface types may have similar or overlapping spectral signatures in the four bands of the multispectral scanner. The desire to distinguish surfaces which are confused (virtually identical in terms of their four-band spectral response) leads naturally to an increase in the number of spectral channels in order to gain additional factors for discrimination. Data from the thermal infrared channel are considered in this context.

It should be pointed out that an alternative approach is available for the analysis of thermal infrared data. The temperature behavior at the Earth's surface results from the balance of radient, latent, sensible, and ground heat fluxes. This temperature behavior is readily susceptible to numerical modeling (Watson, 1975; Rosema, 1975), leading to the possibility of quantitative inferences about surface conditions (Pohn *et al.*, 1974; Price, 1980). Such an approach, though feasible, is quite different from the essentially empirical treatment which is carried out here. Clearly, research along both lines is desirable.

This paper discusses the contribution of the thermal infrared channel (10.4 to 12.6 μm) of Landsat 3 in the classification of a scene acquired over New York State. The next section describes briefly the sensor characteristics and the statistical properties of the five channels of data. The third section presents the conclusions from classification of the scene using four reflective channels

* Now with the Hydrology Laboratory, U.S. Dept. of Agriculture, Beltsville, MD 20705.

PHOTOGRAMMETRIC ENGINEERING AND REMOTE SENSING,
Vol. 47, No. 2, February 1981, pp. 229-236.

(bands 4, 5, 6, and 7) and these four in combination with the emissive band (8). The physical basis of the results is described in the next to last section, and conclusions are summarized in the final section.

Properties of the Data

The characteristics of the multispectral scanner (MSS) on Landsats 1 to 3 have been described elsewhere (General Electric Space Division, 1978; USGS, 1979). For the present study, the essential properties are the spectral characteristics; i.e., four spectral bands at 0.5 to 0.6 μm, 0.6 to 0.7 μm, 0.7 to 0.8 μm, and 0.8 to 1.1 μm, and the spatial resolution at the ground (79 by 79 m) for Landsats 1 and 2. The Landsat 3 MSS acquires additional data in the thermal infrared at 10.4 to 12.6 μm. Due to considerations of lower incident energy and detector sensitivity, the field of view of the thermal channel is 237 by 237 m. As a result, a single thermal-band measurement corresponds to an area represented by nine measurements in each of the original four spectral bands. Both the reflective bands and thermal-IR band are oversampled crosstrack (perpendicular to the direction of satellite motion), but the 9:1 ratio is retained by maintaining the same degree of oversampling.

Data in the thermal band are digitized to six-bit accuracy (0 to 63) over a range of incident energies corresponding to the temperature interval 260 to 340°K. This equates to a quantization interval of approximately 1.2°K at 300°K, or 1.5°K at 280°K. In addition, the precision of the data is affected by noise in the detectors and amplifier circuits prior to digitization.

Unfortunately, the Landsat 3 thermal band did not function properly due to several unexpected causes. Rapid outgassing from within the instrument caused plating of contaminants on the thermal detectors, with a resultant gradual loss of detector sensitivity. The decrease in detector output voltages was corrected by a compensating increase in the gain of the preamplifier circuitry, at the expense of a corresponding decrease in the signal-to-noise ratio. When the maximum gain setting became insufficient to provide adequate voltage output, the instrument was put through a heating cycle that drove off the material on the detectors and restored sensitivity. During the seventh such cycle, one of the two thermal detectors failed after four months of operation.

A second defect occurred in a circuit defining the zero setting of the relationship between scene radiance and detector output. This resulted in a noticeable striping of the data, due to both the differing performance of the two thermal detectors (along track effect) and an apparent change in sensitivity as the detectors swept perpendicular to the satellite motion (across-track effect). These effects were reduced in the image to be discussed through a light smoothing of the thermal data.

The data selected for study were acquired on 18 April 1978 over southeastern New York State (scene center 74° 24′ west, 41° 36′ north). The image was selected for its variety of surface characteristics, including low mountains, turbid water, clear water, snow, a large city, small patches of vegetation, and a few scattered clouds (Figure 1). On this date, the thermal channel (Figure 2) was in gain step 4 during the second day following a four-day outgassing cycle. An apparent noise figure (digitization plus detector) of 1.5°K at 280°K was obtained by assessing the variability in a small area which showed no evidence of temperature gradients (a central portion of Long Island Sound). Figure 3 displays the histogram of the thermal data for the entire image, showing that relatively few levels are available for signature separation during the classification procedure. Five levels represent 71 percent of the image area; nine levels represent more than 90 percent. The low variability of approximately 15°C in the thermal image is ascribed to the time and season of image acquisition; 10:00 A.M. local time, early spring. The temperature contrast would be considerably greater (order 40 to 60 percent) for observations during the early afternoon in midsummer. In addition, the low spatial resolution tends to average out thermal contrast.

The differing fields of view of the original Landsat channels (bands 4 to 7) and the thermal channel (band 8) necessitates a procedure regarding the treatment of the data.

In the present study, it appears that a single band 8 measurement would be of little value in differentiation or classification of the nine higher resolution pixels nested within it. Accordingly, the band 4 to 7 data were averaged to yield pixels equivalent to the band 8 data, despite a significant reduction in the variability of the data. As shown in Table 1, the 9:1 averaging greatly reduces the potential for discrimination of spectral signatures: many of the large pixels evidently are averages of subareas representing differing surface characteristics. However, this degradation does not affect the objectives of this study, i.e., to determine the contribution of the band 8 data in multispectral classification. As a compensating benefit, the reduction in data volume permitted quantitative study of the entire scene.

The effect of averaging was further analyzed through computation of the band-to-band correlation matrices and reduction to principal components for both low and high spatial resolution data. In addition, this permitted assessment of the statistical correlation between the emissive band and the four reflective bands.

Table 2 presents the correlation matrix for the

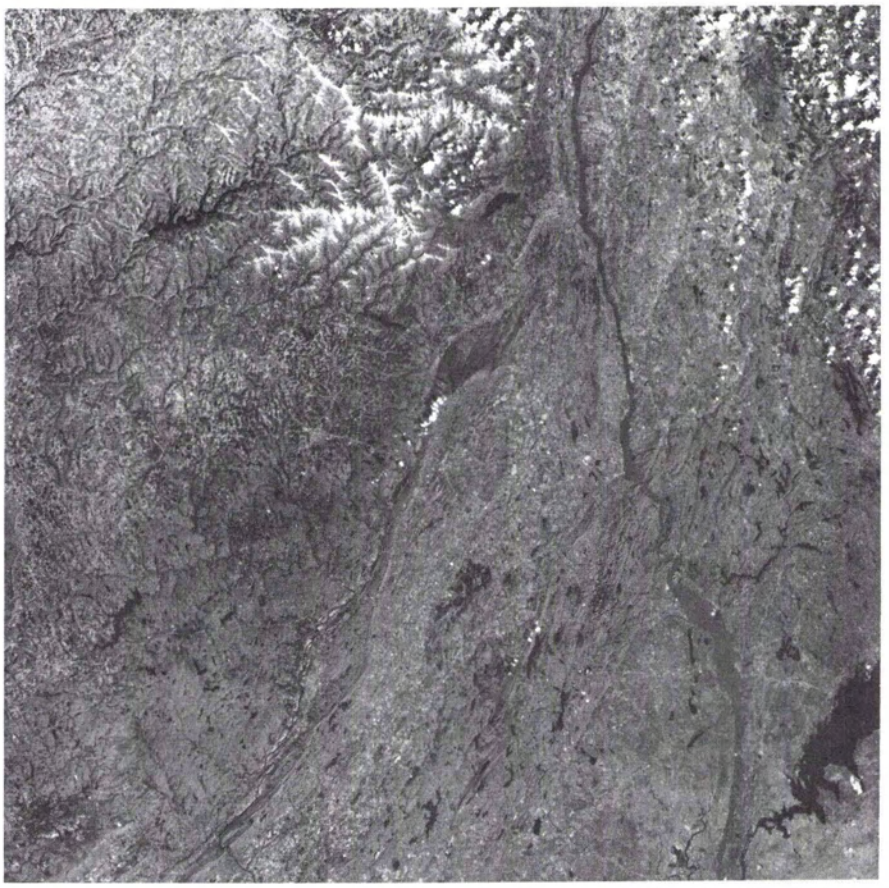

FIG. 1. Landsat visible (band 5) image of southeastern New York State. The Hudson River runs down the right center of the scene. The tip of Long Island South is visible at the lower right.

four-channel 79-metre data. The eigenvectors resulting from the principal axis transformation are displayed in Figure 4. As expected, the variability associated with the dominant eigenvector represents all four spectral intervals having the same sign and nearly the same magnitude. The eigenvector is thus roughly equivalent to a broadband (0.5 to 1.1 μm) reflectivity measurement. The second ranked eigenvector is associated with the contrast between the short wavelength measurements of bands 4 and 5 and the longer wavelength measurements in bands 6 and 7; i.e., a signature typical of vegetation.

Table 3 and Figure 5 present equivalent information for the five-channel low spatial resolution data. Several features are evident:

- The spatial averaging greatly increases the correlations between the visible near-IR channels.
- The correlation of the band 8 data with other bands is strikingly low. It is apparent that this band does, indeed, contain independent information.
- The five-channel eigenvectors are closely similar to those of the original four channels. The second eigenvector is new, being predominately associated with the band 8 data. (It is true that eigenvectors 2 and 3 are similar in bands 4-7. In this sense 2 and 3 represent a partitioning of the number 2 eigenvector in the 4 channel data. However, the band 8 component contributes $e_5^2 = 83.7$ percent of the spectral signature to number 2, while $e_5^2 = 15.8$ percent of the number 3 eigenvector.) The others are essentially unaffected, except that the third and fourth eigenvectors in the high resolution data are interchanged, becoming the fourth and fifth in the low resolution data.

Since the thermal-IR channel is relatively uncorrelated with the others, one may anticipate some impact on the classification procedure.

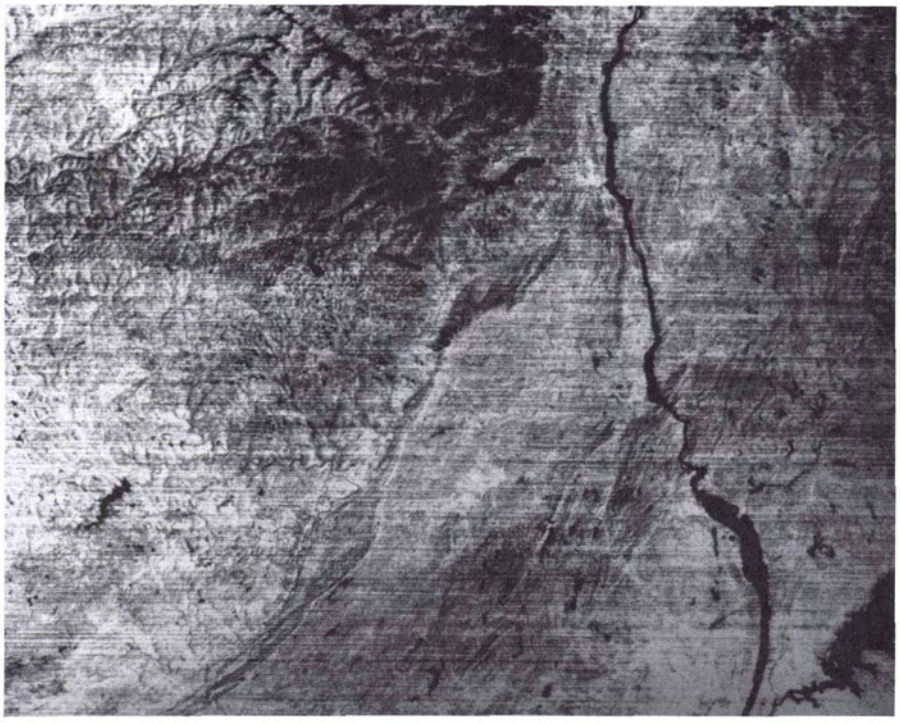

FIG. 2. Thermal-infrared (band 8) image corresponding to Figure 1. The aspect has not been corrected during conversion from computer tape to image following digital contrast enhancement.

CLASSIFICATION OF THE IMAGE DATA

The classification of the five channel low-resolution scene was carried out on an interactive display system (GE Image 100) that uses parallelepiped spectral signatures obtained from training areas. Where necessary, spectral signatures were built up through summation of signatures from several training sites. (In symbolic logic, the operation is designated as "or" (Copi, 1954).) Training-site selection was aided by the use of maps, but was affected mainly through previous familiarity with image classification. A rigorous partitioning was felt to be unnecessary, both because the principal goal was to identify the incremental value of the band 8 data and because the thermal data properties described in the previous section introduced considerable randomness ("noise") into the results for five-channel classification. The 240 by 240 m effective resolution element would make comparison with ground truth data somewhat speculative in any event.

Initially, the band 4 to 7 image data were classified into the following surface types with some uncertainty and ambiguity as noted in the following paragraphs. Because surface-truth information was not readily available (the area in question being a full Landsat frame representing more than 3×10^5 km^2), the classification was carried out subjectively based on differences in the total reflectivity and in the color tones in the image. The differing surface types are listed in approximate order of increasing reflectivity:

(1) Open water (Long Island Sound and some lakes, upper Hudson River);
(2) Clear water in some lakes, cloud shadows on ground, and saturated organic soils (south of Middletown, New York);
(3) Turbid water (mostly lower Hudson River);
(4) Dense urban areas (New York City and nearby cities);
(5) Suburbs of New York City and smaller cities;
(6) Vegetation (mostly parks and undeveloped areas in and near New York City);
(7) Soil, rocks, and dormant vegetation (low reflectivity);
(8) Soil, rocks, and dormant vegetation (higher reflectivity);
(9) Soil, rocks, dormant vegetation, and evergreen vegetation;
(10) Snow; and
(11) Clouds.

Theme 2 definitely represents a mixture of differing surface types. The distinction between themes 7, 8, and 9 is essentially arbitrary, as the spectral signatures vary continuously over the

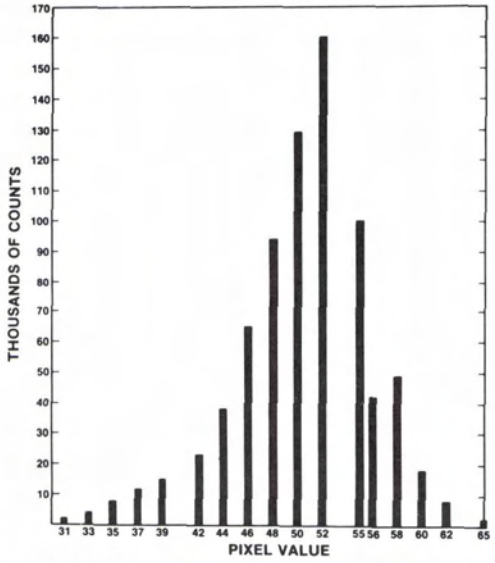

FIG. 3. Histogram of the thermal data. During processing the six-bit (0-63) data are expanded to seven bits (0-127), leading to some spacing between permitted valves.

large areas of wilderness and dormant farmland representing the majority of the scene. The separation of populated areas into themes 4 and 5 also results from a subjective choice of threshold spectral values. Finally, themes 10 and 11 have some spectral overlap, due mainly to the mixed pixel effect at the borders of otherwise highly reflecting clouds.

Following the completion of the classification using bands 4 to 7, the incremental value of the thermal data was studied. For each previously defined theme, the thermal signature was obtained by the appropriate training procedure. Although the small number of possible digital values in the thermal channel would suggest some ambiguity in the thermal signatures, this tendency is in fact quite pronounced, as displayed in Figure 6. In this figure, normalized histograms are displayed for the 11 themes. The substantial spectral overlap or confusion suggests that the thermal signature by itself is less specific to surface type than are the four-channel, visible near-IR signatures. Of course, this is partially due to the "noisy" character of the data. However, this does not preclude the use of band 8 data for further separation of the four-channel themes. To test this possibility, each of the 11 themes was partitioned into two domains representing lower (colder) and higher (warmer) ranges of thermal values. The threshold digital value used to separate cold and warm subthemes was then varied in an effort to optimize the subdivision into recognizably distinct surface classes. The combined effects of relatively low spatial resolution, low thermal sensitivity, and high instrument noise made the exercise qualitative, at best. Nevertheless, the utility of the thermal data for discrimination was apparent in a number of categories (Table 4).

TABLE 2. CORRELATION MATRIX (SYMMETRIC) FOR THE FOUR-CHANNEL HIGH-RESOLUTION LANDSAT DATA

Band	4	5	6	7
4	1.00	0.75	0.51	0.15
5		1.00	0.74	0.42
6			1.00	0.68
7				1.00

In only two cases was the thermal subdivision indicative of a difference of surface type. For theme 2, the thermal signature permitted the distinction of water, which has a moderate and relatively constant temperature throughout the day, from cloud-shadowed areas that remain in the cold predawn condition when direct solar radiation is intercepted by clouds. In the case of theme 11, the tops of the low cumulus clouds present in the scene were measureably colder than the snow present on the top of some mountain ridges.

In all other cases, the thermal data either were not useful (i.e., themes 3, 6, 7, and 8) or were associated with a physically parameter that is not directly related to surface type (themes 1, 4, 5, 9, and 10). Separation of the latter into subthemes would be quite subjective in the sense that a well-defined threshold or spectral boundary for partitioning does not exist. Physical arguments suggest that factors other than the surface type must be considered. In the next section, these factors are discussed and a general interpretation of Landsat thermal data is suggested.

TABLE 1. STATISTICAL PROPERTIES OF THE HIGH- AND LOW-RESOLUTION DATA

Band	Mean (counts)	Standard Deviation (high spatial resolution)	Standard Deviation (low spatial resolution)
4	24.6	12.4	6.3
5	25.6	13.5	7.9
6	35.9	14.7	9.8
7	17.3	11.6	4.7
8	49.5		5.6

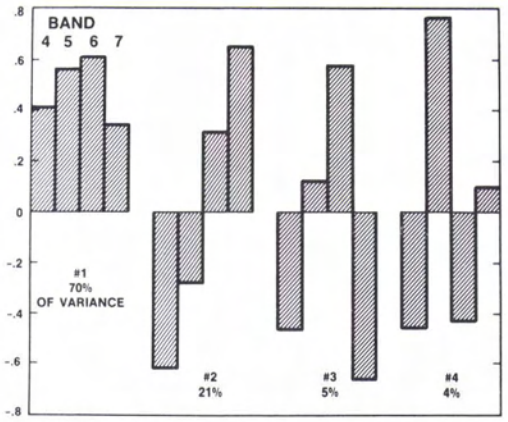

FIG. 4. Spectral eigenvectors for high-resolution (79 m) data. Eigenvectors are normalized such that the sum of the squares of the components is unity.

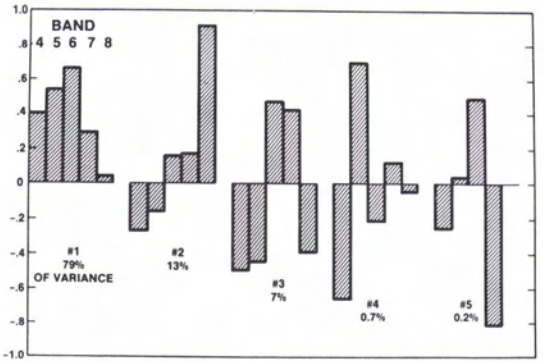

FIG. 5. Spectral eigenvectors for low-resolution (237 m) data. Eigenvectors are normalized such that the sum of the squares of the components is unity.

A PHYSICAL EXPLANATION

The explanation for the relatively low utility of thermal data in multispectral classification involves the differing source of the observed radiation in the visible near-IR channels (bands 4 to 7) versus that in the thermal-infrared (band 8). In general terms, bands 4 to 7 represent reflected solar energy, while band 8 is dominated by thermal emission from the Earth's surface. Quantitative verification may be obtained through evaluation of approximate expressions for the radiance measured by the satellite in the respective spectral intervals. As a first approximation atmospheric effects may be neglected in both intervals. Reflected solar radiation at wavelength λ may be approximated by

$$R_{SUN}(\lambda) = B(\lambda, T_{SUN})(R/L)^2 \, a(\lambda) \cos \eta \text{ watts/m}^2\text{/ster}$$

where B is the Planck function, T_{SUN} is the sun's apparent temperature (5700 K), R/L is the ratio of the sun's radius to the Earth-sun distance, a is the albedo, and η is the solar nadir angle. The radiance due to thermal emission is given by $R_{EARTH}(\lambda) = \epsilon(\lambda)B(\lambda, T_{EARTH})$, where ϵ is the surface emissivity. Numerical results are obtained through substitution of representative values leading to the estimates (R_{SUN}, reflected)/(R_{EARTH}, emitted) $\approx 10^{20}$ at 0.8 μm, (R_{SUN}, reflected)/(R_{EARTH}, emitted) $\approx 3 \times 10^{-4}$ at 11.5 μm. The ratios provide the quantitative basis for ignoring the effect of emitted radiation in the shorter wavelength interval, and for ignoring reflected sunlight in the thermal infrared. The situation in the two wavelength ranges is shown in Figure 7. In the visible near-infrared, the intensity of reflected solar radiation depends principally on the intrinsic reflective characteristics of the surface being imaged. The intensity of reflected radiation is also somewhat dependent on the aspect of the surface because the slope and direction of the slope affect the angle between the sun's rays and the surface. In multispectral classification, this effect of topographic variation may be reduced through the use of band-ratioed data (e.g., 4/5, 5/6, 6/7) instead of the original data with resultant cancellation of the geometric factor. If several thermal-IR channels were available, a similar improvement could be expected by ratioing these bands (Smith, 1977). In the visible near-infrared ratioing leaves variability

TABLE 3. CORRELATION MATRIX FOR THE FIVE-CHANNEL LOW-RESOLUTION DATA

Band	4	5	6	7	8
4	1.00	0.95	0.79	0.63	−0.05
5		1.00	0.87	0.75	0.04
6			1.00	0.96	0.13
7				1.00	0.19
8					1.00

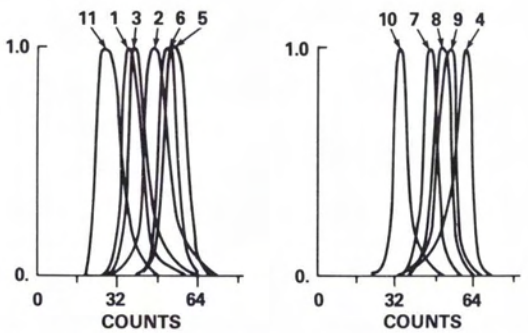

FIG. 6. Histogram of thermal data representing the 11 themes indicated in the text. Each histogram is normalized to unit amplitude. The figure has been split into two parts for purposes of illustration.

TABLE 4. CHARACTERISTICS OF "COLD" AND "WARM" SUBTHEMES AS DETERMINED USING BAND 8 DATA

Theme	Surface Type	Cold Subtheme	Warm Subtheme
1	Clear Water	Center of Long Island Sound	Rivers, shallow areas in Long Island Sound
2	Water, cloud shadows, saturated soil	Cloud Shadows	Water, saturated soils are warmest
3	Turbid water	No separation-striping due to line-to-line jitter	
4	Urban areas	Lower population density	Higher population density industrial areas, commercial
5	Suburbs, small cities	Lower population density	Higher population density, commercial areas
6	Vegetation	No separation	
7	Soil, rocks, dormant vegetation	No separation	
8	Soil rocks, dormant vegetation	No separation	
9	Soil, rocks, evergreen vegetation	Higher elevation in mountains	Lower elevation
10	Snow	Highest areas in mountains	Lower elevations
11	Clouds (some snow)	Clouds	Snow and cloud edges

associated with nonuniformity of bidirectional reflectance as the only evidence of topographic effects.

The explanation for the satellite-observed radiance in the thermal-infrared region of the spectrum is much more complex. Emitted radiation is a function of surface temperature, which results from the balance among a number of energy fluxes, as illustrated in Figure 7.

Surface temperature is only slightly affected by the visible near-IR albedo in bands 4 to 7 because, for a representative range of albedos (10 to 30 percent), the major portion of the solar flux is absorbed. All other fluxes at the Earth's surface can vary substantially, independent of the surface reflective characteristics. The chief variables affecting surface temperatures are:

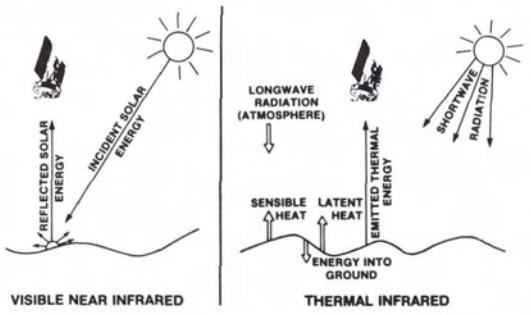

FIG. 7. Factors influencing satellite-observed radiation in the reflective and emissive wavelengths.

(1) *Sky-emitted radiation.* This energy flux depends on the vertically decreasing moisture content of the atmosphere. As a consequence, surface temperature is generally related to elevation, with higher locations being cooler than low-lying areas. The tendency is quite pronounced in the present scene with snow present only on the highest (1300 m) elevations.

(2) *Heat flux into the surface.* This flux is related to the density, heat capacity, and thermal conductivity of the near-surface layer, which are functions of the surface type and hence presumably related to the visible near-IR spectral signature. However, this flux is also related to the surface slope. At the 10 A.M. Landsat overpass time, the surface temperature is typically increasing rapidly as the sun rises higher in the sky. The phase of the diurnal temperature variation is affected by the surface properties response to the incident solar flux, which depends on surface slope. Thus an east-facing slope will by warmer at this time than a west-facing slope, other things being equal. The phase lag between incident heat flux and surface temperature is itself a function of the surface material properties (Watson, 1975). However, it is also dependent on the relative magnitude of heat transfer to the atmosphere as compared to ground heat flux. This phase variability of the surface temperature change causes the time of measurement to be less than optimum for Landsat.

(3) Sensible and latent heat transfer to the atmosphere. These fluxes depend on windspeed, air

temperature, and humidity near the surface; vegetative cover; surface roughness; and availability of water for evapotranspiration. In fact, the cooling effect of evapotranspiration can be species dependent, yielding a dependence of satellite observed temperature on the type of vegetative cover. This effect was not evident in the early spring scene which was studied. It may be possible to regard meteorological factors as reasonably constant over a Landsat-size area if the terrain is sufficiently flat. However, surface characteristics can vary and thus affect surface temperature even for a given surface type (tall trees, short trees, wet soil, dry soil, etc.). Idso *et al.* (1975) have suggested the use of abledo measurements to infer near-surface soil moisture, but only under idealized conditions.

In summary, it is clear that different physical mechanisms come into play in establishing the radiances observed by Landsat in the reflective channels and in the thermal IR. The thermal IR signature (surface temperature) is not a simple function of surface type, but instead is related to the physical processes involved in the surface energy budget.

Conclusion

The thermal channel on the Landsat 3 multispectral scanner acquires new and statistically independent information that is valuable for mapping the thermal characteristics of the Earth's surface. However, the numerous physical processes governing thermal radiation lead to a dependence on surface slope, altitude, and surface energy-balance effects such as ground heat flux, atmospheric heating, and surface evaporation. These effects do not influence the spectral behavior in the reflective channels. Instead, the band 4 to 7 data are simply characterized as resulting from the reflective properties of the area imaged. Because of the differing physical properties of the thermal data, its use in classification is subject to ambiguities and dependencies on other factors that make analysis prone to error. In effect, the thermal data may introduce "noise" in a classification sense. Indiscriminate use of the thermal data as an adjunct to the visible near-IR data appears to be undesirable because of many possibilities for misinterpretation and the fact that the thermal "signature" is not a direct indicator of surface type.

Acknowledgment

I am indebted to Ms. Tina Lien for assistance with the image processing.

References

Copi, I. M., 1954. *Symbolic Logic,* MacMillan Company, New York, New York, p. 13.

General Electric Space Division, 1978. *Landsat 3 Reference Manual,* Philadelphia, Pennsylvania, 213 pages.

Harding, R. A., and R. B. Scott, 1978. *Forest Inventory with Landsat,* State of Washington, Department of Natural Resources, Olympia, Washington, 221 pages.

Idso, S. B., R. D. Jackson, R. J. Reginato, B. A. Kimball, and F. S. Nakayama, 1975. The Dependence of Bare Soil Albedo on Soil Water Content, *J. Applied Meteorology,* Vol. 14, pp. 109-113.

Pohn, H. A., T. W. Offield, and K. Watson, 1974. Thermal Inertial Mapping from Satellites—Discrimination of Geologic Units in Oman, *Journal Research, U.S. Geological Survey,* 2 (2), pp. 147-158.

Price, J. C., 1980. The Potential of Remotely Sensed Thermal Infrared Data to Infer Surface Soil Moisture and Evaporation, *Water Resources Research,* Vol. 16, pp. 787-795.

Rabchevsky, G. A., U. P. Boegli, and J. Valdes, 1979. Landsat Geologic Reconnaissance of the Washington, D.C. Area Westward to the Appalachians, *Photogrammetric Engineering and Remote Sensing,* Vol. 45, No. 2, pp. 611-621.

Rosema, A., 1975. *A Mathematical Model for Simulation of the Thermal Behavior of Bare Soils Based on Heat and Moisture Transfer,* Rep. 11, Neth. Interdepartmental Work, Community for the Appl. of Remote Sensing Tech., Delft, Netherlands.

Scarpace, F. L., K. W. Holmquist, and L. T. Fisher, 1979. Landsat Analysis of Lake Quality, *Photogrammetric Engineering and Remote Sensing,* Vol. 45, No. 5, pp 623-633.

Smith, W. L., 1977. *Remote Sensing Applications for Mineral Exploration,* Dowdon, Hutchinson, and Ross, Chapter 10.

Thompson, D. R., and O. A. Wehmanen, 1979. Using Landsat Digital Data to Detect Moisture Stress, *Photogrammetric Engineering and Remote Sensing,* Vol. 45, No. 2, pp 201-207.

U.S. Geological Survey, 1979. *Landsat Data User's Handbook,* 3rd Edition.

Watson, K., 1975. Geologic Applications of Thermal Infrared Imagery, *Proceedings of IEEE,* Vol. 63, pp 128-137.

(Received 22 January 1980; revised and accepted 30 August 1980)